JOURNAL OF SOLID STATE CHEMISTRY 30, 35–44 (1979)

Crystal Structures and Crystal Chemistry of the RETiO$_3$ Perovskites: RE = La, Nd, Sm, Gd, Y

DAVID A. MacLEAN, HOK-NAM NG, AND J. E. GREEDAN

Department of Chemistry and Institute for Materials Research, McMaster University, Hamilton, Ontario, L8S 4M1, Canada

Received August 23, 1978

The structures of the RETiO$_3$ perovskites, RE = La, Nd, Sm, Gd, and Y, were solved using single-crystal, automated diffractometer techniques. All were found to belong to space group *Pbnm* and are, therefore, isostructural with the REFeO$_3$ perovskites. The structure of LaTiO$_3$ was solved using a crystal exhibiting a complex twinning. The RE–O and Ti–O coordination polyhedra were studied as a function of the RE ion and were compared with those for REFeO$_3$. The major difference in results between RETiO$_3$ and REFeO$_3$ is a more highly distorted Ti–O octahedron for RE = Gd and Y.

Introduction

The problem of the structure of the rare-earth titanium(III) oxides, RETiO$_3$, is one of long standing. The contents of Table I provide an historical account of the existing structural data for the materials studied here. Confusion has persisted regarding even the true crystal system of those compounds for which RE = La to Sm, the so-called light rare earths. Various authors, working with powder data, have reported cubic, psuedo-cubic, or orthorhombic cells. There is less disagreement regarding the compounds for RE = Gd to Lu. (The phase EuTiO$_3$, an Eu(II)Ti(IV) compound, is not properly a member of this structural series.) Following the original work by Geller (*8*) on GdFeO$_3$, the powder patterns of this series have been indexed on an orthorhombic cell of probable space group *Pbnm*. There is generally poor agreement between cell constants reported by different authors for the same materials.

To clarify this situation we undertook to determine the structure of selected members of the RETiO$_3$ series using single-crystal data obtained with automated diffractometer techniques. Our intention was to obtain data of sufficient quality to permit comparison with the very careful work of Marezio *et al.* on the REFeO$_3$ phases (*9*).

In addition to the existing confusion regarding crystal data for the RETiO$_3$ compounds, there is convincing evidence that their physical properties depend strongly on the size of the rare earth ion. For example, LaTiO$_3$ is metallic and Pauli paramagnetic while YTiO$_3$ is semiconducting and ferromagnetic (*10*). According to arguments by Goodenough (*11*), these properties may be structurally controlled. In a subsequent publication we shall report on some of the properties of these phases, pointing out correlations with the structural details.

0022-4596/79/100035-10$02.00/0

TABLE I

CRYSTAL DATA FOR RETiO$_3$: A HISTORY RE = La, Nd, Sm, Gd, Y

RE	Symmetry	Cell constants (Å)	Year	Reference
	Cubic	$a = 3.92$	1954	(*1*)
	Pseudocubic	$a \approx 3.89$	1956	(*2*)
	Orthorhombic	$a = b = 5.596$	1961	(*3*)
La		$c = 7.914$		
	Orthorhombic	$a = 5.54$		
		$b = 5.75$	1966	(*4*)
		$c = 7.83$		
	Cubic	$a = 3.92$	1976	(*5*)
	Pseudocubic	$a = 3.90$	1956	(*2*)
	Orthorhombic	$a = 5.48$		
		$b = 5.70$	1966	(*4*)
Nd		$c = 7.76$		
	Cubic	$a = 3.87$	1976	(*5*)
	Pseudocubic	$a \approx 3.88$	1956	(*2*)
	Orthorhombic	$a = 5.398$		
		$b = 5.568$	1969	(*6*)
Sm		$c = 7.651$		
	Cubic	$a = 3.86$	1976	(*5*)
	Orthorhombic	$a = 5.44$		
		$b = 5.56$	1966	(*4*)
Gd		$c = 7.43$		
	Orthorhombic	$a = 5.353$		
		$b = 5.655$	1969	(*6*)
		$c = 7.616$		
	Orthorhombic	$a = 5.340$		
		$b = 5.665$	1969	(*6*)
Y		$c = 7.624$		
	Orthorhombic	$a = 5.327$		
		$b = 5.618$	1973	(*7*)
		$c = 7.591$		

Experimental

Crystal Growth

The RETiO$_3$ phases were prepared by reacting equimolar quantities of the rare earth and titanium sesquioxides. Ti_2O_3 was prepared by arc melting Ti sponge (99.99%) and TiO_2 (99.95%) in a purified Ar/He atmosphere. Stoichiometry could be controlled to an O/Ti = 1.500 ± 0.005 and was monitored using tga. Trace impurity levels were below 100 ppm as determined by emission spectrographic data. The rare earth sesquioxides were prefired at 1000°C before use.

All crystals were grown from the melt in molybdenum crucibles under a purified argon atmosphere using rf heating. All RETiO$_3$ compounds appear to melt congruently in the range from 2080 ± 20°C for RE = La to 1960 ± 20°C for RE = Y. Full details of the crystal growth will be described in a subsequent publication. A crystal of $YTiO_3$, ~3 mm largest dimension, was grown by the Czochralski technique. $LaTiO_3$, $SmTiO_3$, and $GdTiO_3$ crystals of a similar size were grown in open crucibles at a cooling rate of 50°C/hr. $NdTiO_3$ was grown in both open and welded crucibles using a cooling rate near 3°/hr. Cell constants for the two batches of $NdTiO_3$ were identical to within experimental error. Analysis of the materials was done by a combination of tga and neutron activation, when possible. The data are given below.

Crystal Data

Precession photographs of untwinned crystals of the RETiO$_3$ series showed that the conditions of systematic absences were $h + l \neq 2n$ for $h0l$, $k \neq 2n$ for $0kl$, $h \neq 2n$ for $h00$, $k \neq 2n$ for $0k0$ and $l \neq 2n$ for $00l$. The orthorhombic centric space group *Pbnm* was

TABLE II

ANALYTICAL DATA RETiO$_3$

	tga (mg)		
RE	Wt gain (expt)	Wt gain (theor)	Neutron activation (RE : Ti)
La	0.710	0.727	—
Nd	0.809	0.822	1 : 1.025
Sm	0.698	0.714	1 : 1.025
Gd	0.734	0.747	—
Y	1.085	1.104	—

chosen for initial refinement over the acentric $Pbn2_1$ both from a consideration of the statistical distribution of intensities and from an expectation that the $RETiO_3$ would be isostructural with the $REFeO_3$, which are known to be best described in space group $Pbnm$ (*8*). There are four formula units per unit cell. The 4 rare earth atoms are in the special positions 4(*c*) $(x, y, \frac{1}{4})$, the 4 iron atoms are in the special positions 4(*b*) $(0, \frac{1}{2}, 0)$, 4 of the 12 oxygen atoms are in the special positions 4*c* $(x, y, \frac{1}{4})$, and 8 are in general positions. Accurate unit-cell parameters, reported in Table III, were obtained by a least-squares refinement of the 2θ values $(20° < 2\theta < 35°)$ of 15 reflections carefully measured on the diffractometer.

Intensity Measurements

For collection of intensity data, all crystals were ground to spherical shape. Data were collected on two Syntex automatic diffractmeters, Models $P\bar{1}$ and $P2_1$, in the $\theta/2\theta$ scan mode using graphite-monochomatized Mo$K\alpha$ radiation ($\lambda = 0.71069$ Å) and a scintillation detector. Reflections were scanned at variable rates from 4.0 to 24.0°/min in 2θ to minimize counting errors for the weak reflections. Reflections for each crystal were collected within a sphere defined by 2θ given in Table IV. Reflections whose intensity, corrected for background, were less than three times the standard deviation were considered unobserved. Equivalent reflections (after any correction or omission for twinning, if necessary) were averaged, and the data were corrected for Lorentz and polarization effects. Absorption corrections were also applied in each case assuming spherical shape (radii and linear absorption coefficients are given in Tables IV and III).

Twinning

Precession photographs showed that the crystals of $SmTiO_3$ and $NdTiO_3$ used for data components, and a plot of the intensities of found to correspond to a reflection across the $(1\bar{1}0)$ plane. For $SmTiO_3$, intensity data were collected separately for the two twin components, and a plot of the intentsitites of the twin-related reflections revealed a volume ratio of 4.4:1. Only the data for the major component were used. The intensities of the hhl reflections ($h \neq 0$), which were superimposed because of twinning, were not used in the refinement; rather the equivalent, nonsuperimposed $h\bar{h}l$ reflections were used. The intensities of the $00l$ reflections were reduced by a factor of 4.4/5.4 before being used in the refinement. In the case of $NdTiO_3$, the volume ratio was found to be 10.8:1, and the data were handled in a manner identical to that of $SmTiO_3$.

TABLE III

$RETiO_3$ CRYSTAL DATA[a]

	La	Nd	Sm	Gd	Y
a (Å)	5.601(2)	5.495(3)	5.454(2)	5.393(2)	5.316(2)
b (Å)	5.590(2)	5.589(3)	5.660(2)	5.691(2)	5.679(2)
c (Å)	7.906(4)	7.779(4)	7.722(4)	7.664(3)	7.611(3)
V (Å^3)	247.5(2)	238.9(2)	238.4(2)	235.2(2)	229.8(2)
μ[b] (cm^{-1})	203.5	246.6	279.6	320.5	292.3
ρ_{calcd} (g/cm^3)	6.30	6.68	6.86	7.15	5.34
ρ_{exptl} (g/cm^3)	6.25	6.65	6.83	7.13	5.31

[a] Standard deviations given in parantheses.
[b] Linear absorption coefficient.

TABLE IV
DATA COLLECTION AND REFINEMENT INFORMATION

	Crystal radius (mm)	μR	Data collected to 2θ of (deg)	Weighting scheme coefficients[a]			$N(1)$	$N(2)$	N	R	ωR[b]
				A	B	C					
La	0.142	2.90	70.0	3.608	−0.029	0.0001	293	231	273	0.050	0.044
Nd	0.149	3.68	65.0	0.759	−0.012	0.0003	463	424	435	0.024	0.032
Sm	0.100	2.79	65.0	3.018	−0.008	0.0007	458	398	414	0.032	0.042
Gd	0.088	2.80	55.0	2.500	−0.063	0.0005	294	282	284	0.015	0.016
Y	0.099	2.88	55.0	6.119	−0.192	0.0017	278	250	264	0.029	0.026

[a] Coefficients are those in the weighting function $\omega = A + BF_0 + CF_0^2)^{-1}$.
[b] $\omega R = \{[\sum \omega(|F_0| - |F_c|)^2]/\sum \omega F_0^2\}^{1/2}$.

The case of $LaTiO_3$ was quite different. Precession photographs revealed a nearly cubic cell, $a \sim 7.91$ Å. Indexed on an orthorhombic basis, the $h0l$ and $0kl$ projections showed obvious violations of the n and b glide plane symmetry, leading one to suspect that the space group was not *Pbnm*. The data for $LaTiO_3$ can be analyzed in terms of *Pbnm*, however, by postulating and proving the existence of a complex twinning. This twinning can be viewed as a combination of two basic operations.

The first and most predominant twin in $LaTiO_3$ corresponds to a threefold rotation about the body diagonal of the 7.91 Å pseudocube. This twinning results in three twin components, whose reflections (indexed in the orthocell) are related by the following transformation matrices:

$$\begin{pmatrix} -\frac{1}{2} & -\frac{1}{2} & -\frac{1}{2} \\ \frac{1}{2} & \frac{1}{2} & -\frac{1}{2} \\ -1 & 1 & 0 \end{pmatrix} \begin{pmatrix} h \\ k \\ l \end{pmatrix} = \begin{pmatrix} h' \\ k' \\ l' \end{pmatrix},$$

$$\begin{pmatrix} \frac{1}{2} & -\frac{1}{2} & \frac{1}{2} \\ \frac{1}{2} & -\frac{1}{2} & -\frac{1}{2} \\ 1 & 1 & 0 \end{pmatrix} \begin{pmatrix} h \\ k \\ l \end{pmatrix} = \begin{pmatrix} h'' \\ k'' \\ l'' \end{pmatrix}.$$

It can be seen that reflections will be superimposed by this twinning only when $h + k + l = 2n$. When $h + k + l \neq 2n$, the twinning causes reciprocal lattice points to appear at half-integral coordinates with respect to the orthorhombic lattice, giving rise to the appearance of a 7.91-Å cubic cell. Thus one can use those reflections for which $h + k + l \neq 2n$ in the structural refinement as they will be nonsuperimposed by twinning.

From a data collection on the 7.91-Å cell, plots were made of the intensities of twin-related reflections, revealing volume ratios of 0.089 : 0.14 : 1. Data were then collected on the orthorhombic cell of the major twin component. Of the data set collected, two types of reflections were used in the refinement. First, as described above, were included those reflections for which $h + k + l \neq 2n$. Also used in the refinement were 29 reflections which contained intensities from the major twin component and the smallest twin component only. These reflections were reduced by a factor of 1/1.089 before being used.

The second twin operation present in $LaTiO_3$ is reflection across the $(1\bar{1}0)$ plane, as was found for $SmTiO_3$ and $NdTiO_3$. In the cases of $SmTiO_3$ and $NdTiO_3$, the a^* and b^* axes were of significantly different lengths so that this twin plane did not cause superimposition of reflections (other than hhl). However, in $LaTiO_3$ the a^* and b^* axes are essentially identical in length, and twinning

TABLE V

FINAL POSITIONAL PARAMETERS AND THERMAL PARAMETERS ($\times 10^4$)[a]

		La	Nd	Sm	Gd	Y
RE	X	0.9949(4)	0.98892(5)	0.98433(9)	0.98103(5)	0.97925(14)
	Y	0.0323(19)	0.05412(6)	0.06444(9)	0.06958(5)	0.07294(12)
	Z	(0.25)	(0.25)	(0.25)	(0.25)	(0.25)
	U_{11}[b]	139(4)	113(2)	105(3)	60(2)	63(4)
	U_{22}	186(16)	131(2)	86(3)	67(2)	37(4)
	U_{33}	124(4)	101(2)	103(3)	64(2)	64(4)
	U_{12}	−15(4)	−8(1)	−5(2)	−6(1)	−6(3)
	U_{13}[c]	(0)	(0)	(0)	(0)	(0)
	U_{23}	(0)	(0)	(0)	(0)	(0)
Ti	X	(0.0)	(0.0)	(0.0)	(0.0)	(0.0)
	Y	(0.5)	(0.5)	(0.5)	(0.5)	(0.5)
	Z	(0.0)	(0.0)	(0.0)	(0.0)	(0.0)
	U_{11}		80(4)	91(7)	51(4)	58(6)
	U_{22}		99(4)	91(4)	64(5)	37(6)
	U_{33}		69(5)	79(7)	39(5)	30(6)
	U_{12}	(U_{ISO}[d] = 86)	0(3)	1(5)	−1(3)	1(5)
	U_{13}		0(2)	0(5)	−5(3)	−10(6)
	U_{23}		−5(4)	0(6)	7(3)	−1(3)
O1	X	0.0696(48)	0.0902(8)	0.1019(13)	0.1095(8)	0.1213(10)
	Y	0.4912(13)	0.4801(8)	0.4735(13)	0.4668(8)	0.4580(9)
	Z	(0.25)	(0.25)	(0.25)	(0.25)	(0.25)
	U_{11}	225(109)	108(17)	109(29)	123(18)	65(24)
	U_{22}	71(65)	154(17)	96(29)	77(19)	43(26)
	U_{33}	295(152)	74(16)	115(32)	62(19)	80(26)
	U_{12}	−41(25)	2(14)	12(23)	0(16)	12(21)
	U_{13}	(0)	(0)	(0)	(0)	(0)
	U_{23}	(0)	(0)	(0)	(0)	(0)
O2	X	0.7150(22)	0.7024(5)	0.6958(8)	0.6942(5)	0.6909(6)
	Y	0.2861(22)	0.2979(5)	0.3022(8)	0.3063(5)	0.3095(7)
	Z	0.0368(15)	0.0465(4)	0.0524(7)	0.0541(4)	0.0579(5)
	U_{11}	199(33)	112(11)	115(18)	63(12)	72(18)
	U_{22}	182(30)	118(11)	66(18)	86(14)	54(19)
	U_{33}	195(36)	124(12)	104(20)	82(14)	78(18)
	U_{12}	−58(31)	−13(9)	−7(15)	−24(10)	−22(14)
	U_{13}	−36(35)	7(9)	25(16)	4(9)	−8(14)
	U_{23}	34(35)	−14(10)	−5(16)	−21(11)	−8(15)

[a] Standard deviations given in parantheses.

[b] Calculated from $\beta_{ij} = 2\pi^2 b_i b_j U_{ij}$, where $T = \exp[-(\beta_{11}h^2 + 2\beta_{12}hk + \cdots)]$ is the thermal factor appearing in the structure factor expression and b_i's are reciprocal lattice vectors.

[c] By symmetry, $U_{13} = U_{23} = 0$ for *RE* and O1.

[d] Temperature parameters for Ti in $LaTiO_3$ were not refined as no reflections containing information about Ti were included in the refinement.

across the $(1\bar{1}0)$ causes direct superimposition of hkl and khl reflections. This aspect of the twinning in $LaTiO_3$ is the same as that found in $LaFeO_3$ (*15*). Intensities were corrected using the formula

$$I_{corr}(hkl) = \frac{1}{1-V} I_{meas}(hkl) - \frac{V}{1-V} I_{meas}(khl),$$

where V is the volume ratio determined by measuring the intensities of the forbidden reflections in the zone $h0l$ and comparing with them the corresponding allowed $0kl$ reflections. For this crystal, the volume ratio was found to be 0.090.

It is interesting to compare the twinning found in $LaTiO_3$ with that for the isostructural $LaFeO_3$. Both crystals show evidence for the $(1\bar{1}0)$ reflection twin but $LaTiO_3$, which was grown from the melt (2000°C), shows a threefold rotational twin while the flux-grown $LaFeO_3$ (1200°C) does not. This suggests that $LaTiO_3$ undergoes a high-temperature phase transition from a rhombohedral or cubic cell to the orthorhombic cell upon cooling.

TABLE VI

INTERATOMIC DISTANCES (Å) AND ANGLES (°) IN THE RARE EARTH POLYHEDRON[a]

	La	Nd	Sm	Gd	Y
RE(2)–O1(1)	2.450(27)	2.349(4)	2.315(7)	2.284(4)	2.221(5)
–O1(2)	3.054(14)	3.256(4)	3.405(7)	3.499(4)	3.573(5)
–O1(3)	3.170(27)	3.209(4)	3.238(7)	3.238(4)	3.259(5)
–O1(4)	2.599(14)	2.445(4)	2.403(7)	2.365(4)	2.314(5)
–O2(1), O2(2)	2.474(14)	2.379(3)	2.345(5)	2.322(3)	2.279(4)
–O2(3), O2(4)	2.704(14)	2.615(3)	2.572(5)	2.542(3)	2.508(4)
–O2(5), O2(6)	2.773(13)	2.717(3)	2.712(5)	2.693(3)	2.684(4)
–02(7), O2(8)	3.309(13)	3.474(3)	3.578(5)	3.616(3)	3.645(4)
O1(1)–*RE*(2)–O1(2)	76.8(6)	70.0(1)	66.3(2)	63.8(1)	60.7(2)
O1(2)–*RE*(2)–O1(3)	93.7(6)	92.4(1)	91.7(2)	91.0(1)	90.7(1)
O1(3)–*RE*(2)–O1(4)	103.4(7)	110.6(1)	114.6(2)	117.4(1)	120.6(1)
O1(4)–*RE*(2)–O1(1)	86.1(7)	87.0(2)	87.4(3)	87.8(2)	88.0(1)
O2(1)–*RE*(2)–O2(2)	85.9(5)	83.4(1)	81.2(2)	80.6(1)	79.8(1)
O2(1)–*RE*(2)–O2(5)	81.8(4)	79.0(1)	78.0(1)	77.5(1)	76.7(1)
O2(2)–*RE*(2)–O2(3)	65.9(4)	69.2(1)	71.9(2)	73.3(1)	74.6(1)
O2(2)–*RE*(2)–O2(7)	57.8(4)	55.5(1)	54.0(1)	53.0(1)	52.2(1)
O2(3)–*RE*(2)–O2(4)	77.1(4)	74.5(1)	72.8(2)	72.4(1)	71.3(1)
O2(3)–*RE*(2)–O2(6)	63.6(4)	65.6(1)	66.7(2)	67.0(1)	67.3(1)
O2(3)–*RE*(2)–O2(7)	98.0(4)	100.8(1)	102.4(1)	103.2(1)	103.8(1)
O2(5)–*RE*(2)–O2(6)	109.7(4)	116.2(1)	118.9(1)	119.9(1)	121.7(1)
O2(6)–*RE*(2)–O2(7)	54.4(4)	53.0(1)	52.6(1)	52.5(1)	52.1(1)
O2(7)–*RE*(2)–O2(8)	86.5(4)	83.2(1)	81.5(1)	80.3(1)	80.0(2)
O1(1)–*RE*(2)–O2(6)	65.9(3)	68.2(1)	69.3(1)	69.8(1)	70.9(1)
O1(1)–*RE*(2)–O2(7)	57.4(4)	54.5(1)	52.8(1)	51.7(1)	50.6(1)
O1(2)–*RE*(2)–O2(2)	60.9(5)	58.8(1)	57.1(1)	56.5(1)	56.1(1)
O1(2)–*RE*(2)–O2(7)	53.1(4)	50.1(1)	48.6(1)	47.5(1)	46.8(1)
O1(3)–*RE*(2)–O2(2)	59.0(3)	59.0(1)	59.1(1)	58.9(1)	58.7(1)
O1(3)–*RE*(2)–O2(3)	57.3(3)	58.0(1)	58.6(1)	59.8(1)	60.6(1)
O1(4)–*RE*(2)–O2(3)	64.9(6)	68.3(1)	70.1(2)	70.8(1)	72.1(1)
O1(4)–*RE*(2)–O2(6)	64.4(4)	66.8(1)	67.6(1)	67.9(1)	68.2(1)

[a] Standard deviations given in parentheses.

Refinements

A full matrix least-squares program that minimizes the function $\sum\omega(|F_0|-|F_c|)^2$ was use in the refinements. The weighting function used has the form $\omega = [A+B|F_0|+C|F_0|^2]^{-1}$ with the coefficients chosen in such a way that the averages of $\omega(\Delta F)^2$ were approximately constant when the data were analyzed into regions of F_0. Atomic scattering curves (for free ions) were taken from Cromer and Waber (*12*) and the real and imaginary anomalous dispersion coefficients were taken from Cromer (*13*). The starting values used for the positional parameters were those of the corresponding REFeO$_3$. During the final stages of refinement, a secondary extinction parameter following Larson (*14*) was also refined in all cases except LaTiO$_3$. The final positional and thermal parameters are listed in Table V. (Tables of structure amplitudes (7 pages) are available from authors upon request).

Discussion

The interatomic distances and angles are given in Tables VI, VII, and VIII. Figure 1 shows a projection of the LaTiO$_3$ structure on the *xy* plane. An oxygen–titanium octahedron and an oxygen–rare earth polyhedron are outlined.

As in the REFeO$_3$, the oxygen polyhedron around the rare earth ions is very distorted. The 12 O–RE–O angles, which in the ideal cubic perovskite are 90°, vary from 121.7 to 60.7° in YTiO$_3$ and from 111.8 to 75.2° in LaTiO$_3$, which has the least distortion of the RETiO$_3$.

The RE–O distances are plotted in Fig. 2 against the crystal radii (*16*) of the rare earths. Over this range of rare earth radii, the first eight RE–O distances increase linearly from Y to La. This indicates that these oxygen atoms are nearest neighbors to the rare earth. The last four RE–O distances are significantly greater and all decrease as a function of the rare earth ionic radius. This indicates that these four atoms are second-nearest neighbors. Thus, over this range of rare earth radii the RETiO$_3$ have an eight-coordinated rare earth ion. These results are similar to those for REFeO$_3$ in every respect.

A different situation arises when one examines the transition-metal–oxygen

TABLE VII

RARE EARTH–TITANIUM DISTANCES (Å) AND Ti–O–Ti AND RE–O–Ti BOND ANGLES (°)[a]

	La	Nd	Sm	Gd	Y
RE(2)–Ti(1), Ti(2)	3.456(2)	3.429(1)	3.431(1)	3.415(1)	3.385(1)
RE(2)–Ti(3), Ti(4)	3.572(9)	3.657(1)	3.734(1)	3.767(1)	3.771(1)
RE(2)–Ti(5), Ti(6)	3.277(9)	3.162(1)	3.132(1)	3.112(1)	3.085(1)
RE(2)–Ti(7), Ti(8)	3.409(2)	3.330(1)	3.292(1)	3.249(1)	3.207(1)
Ti(2)–O1(1)–Ti(1)	157.5(1.5)	150.7(2)	146.8(4)	144.1(2)	140.3(3)
Ti(2)–O2(7)–Ti(4)	156.9(7)	150.3(2)	147.0(3)	145.7(2)	143.7(4)
Ti(1)–O1(1)–RE(2)	101.0(8)	103.5(1)	104.6(2)	105.1(1)	105.7(2)
Ti(1)–O1(1)–RE(1)	88.6(3)	89.9(1)	89.9(2)	90.2(1)	90.4(2)
Ti(4)–O2(2)–RE(1)	91.2(5)	90.6(1)	90.0(2)	88.9(1)	88.2(1)
Ti(1)–O2(5)–RE(2)	91.0(4)	91.6(1)	91.3(2)	91.6(1)	91.0(1)
Ti(5)–O2(5)–RE(2)	84.7(4)	82.1(1)	80.9(2)	80.3(1)	79.7(1)
Ti(7)–O2(1)–RE(1)	86.7(5)	85.0(1)	84.7(2)	85.1(1)	85.2(1)
Ti(8)–O2(1)–RE(2)	98.1(1)	98.1(1)	97.0(2)	96.5(1)	96.4(2)
Ti(3)–O2(1)–RE(2)	104.8(5)	111.7(1)	115.9(2)	117.8(1)	119.9(2)

[a] Standard deviations given in parentheses.

TABLE VIII

INETERATOMIC DISTANCES (Å) AND ANGLES (°) IN THE TITANIUM OCTAHEDRON[a]

	La	Nd	Sm	Gd	Y
Ti–O1(1)	2.015(5)	2.010(1)	2.014(2)	2.014(1)	2.023(2)
Ti–O2(6)	2.016(12)	2.020(3)	2.042(5)	2.027(3)	2.016(4)
Ti–O2(7)	2.023(12)	2.035(5)	2.056(5)	2.076(3)	2.077(4)
O1(1)–O2(6)	2.854(17)	2.856(4)	2.878(7)	2.867(4)	2.869(5)
O1(1)–O2(7)	2.865(15)	2.849(4)	2.855(7)	2.839(4)	2.817(5)
O1(1)–O2(2)	2.846(23)	2.843(5)	2.859(8)	2.847(5)	2.843(6)
O1(1)–O2(3)	2.846(17)	2.872(5)	2.902(8)	2.944(5)	2.979(6)
O2(6)–O2(7)	2.822(17)	2.843(4)	2.891(6)	2.908(4)	2.908(5)
O2(6)–O2(3)	2.889(17)	2.891(4)	2.905(7)	2.893(4)	2.881(5)
O1(1)–Ti(2)–O2(7)	90.4(6)	89.5(2)	89.1(3)	87.9(2)	86.8(2)
O1(1)–Ti(2)–O2(1)	90.2(7)	90.3(2)	90.4(3)	90.4(2)	90.5(2)
O2(7)–Ti(2)–O2(6)	88.7(5)	89.0(1)	89.7(2)	90.3(1)	90.5(1)
Average Ti–O	2.018(10)	2.022(3)	2.037(4)	2.039(3)	2.039(4)
SD of Ti–O	0.0043	0.0126	0.0214	0.0327	0.0334

[a] Standard deviations given in parentheses.

octahedron. In the study of the REFeO$_3$ it was found that the distortion of the Fe–O octahedron was small and increased only slightly in going from LaFeO$_3$ to LuFeO$_3$, the average Fe–O and O–O distances being nearly the same. In the RETiO$_3$, however, a significant distortion of the Ti–O octahedron occurs as a function of the rare earth ion. In Fig. 3, we plot the standard deviation from the mean for the three inequivalent Ti–O bond lengths versus the RE radius in RETiO$_3$ along with those for Fe–O in REFeO$_3$ for comparison. In contrast to the relatively smooth variation for σ (Fe–O),

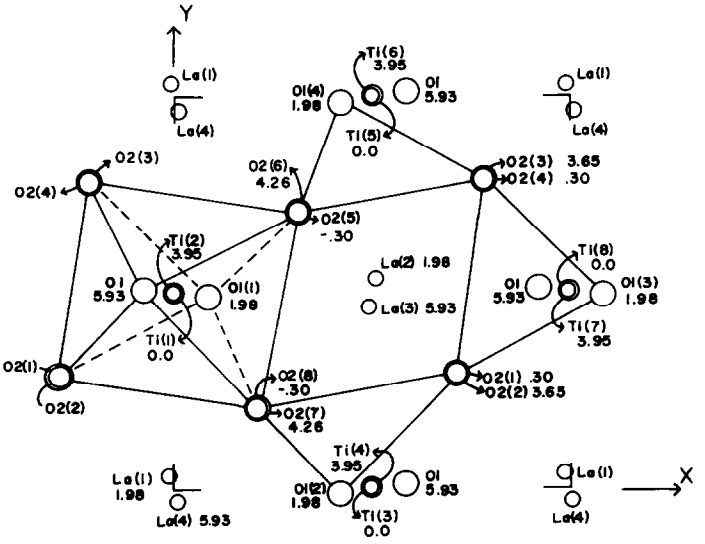

FIG. 1. A projection of the LaTiO$_3$ structure on the xy plane. Position on the z-axis is given in Angstroms.

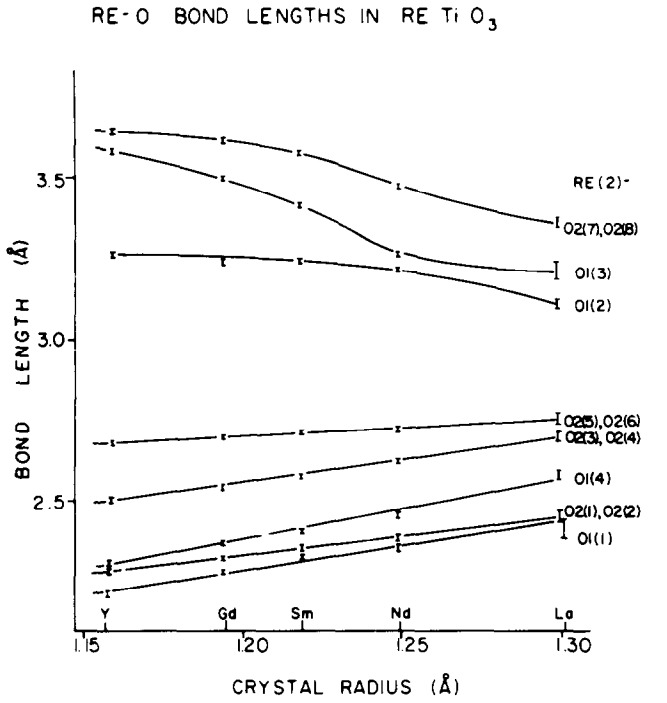

FIG. 2. Variation of the *RE*–O distances with the crystal radius of RE^{3+} (*16*) for nearest and next-nearest neighbors.

σ(Ti–O) shows a sharp increase between *RE* = Nd and *RE* = Gd. The data of Table VIII show that for *RE* = Gd and Y a pronounced tetragonal-like distortion exists with two *trans* Ti–O bonds being much longer than the other four. For *RE* = La the octahedron is undistorted while a very minor, possibly insignificant, distortion occurs for *RE* = Nd. The case for *RE* = Sm is intermediate in character. The origin of this behavior in $RETiO_3$ is at present unclear. We will argue in subsequent publications that the observed structural data are strongly correlated with the magnetic, optical, and electrical properties of these materials.

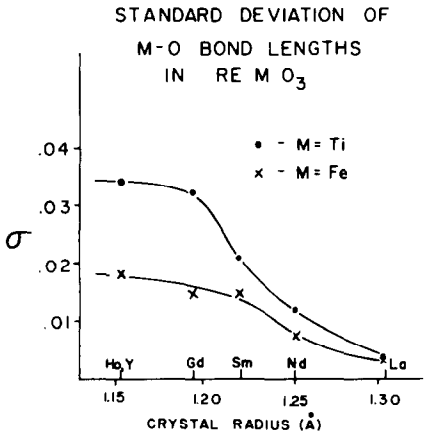

FIG. 3. Standard deviation from the mean for three inequivalent, nearest-neighbor Ti–O distances as a function of the RE^{3+} crystal radius (*16*). Similar data for $REFeO_3$ are shown for comparison (*1, 15*).

Another structural parameter which may be important in the determination of the properties of the $RETiO_3$ phases is the Ti–O–Ti bond angle (*11*). These data are listed in Table VII and plotted in Fig. 4 for both $REFeO_3$ and $RETiO_3$. Note the relatively smooth increases in average bond angle from *RE* = Y, Ho, to *RE* = La for both series, there being no discontinuous changes between *RE* = Y, Gd, and *RE* = La, Nd as found in the Ti–O coordination polyhedron.

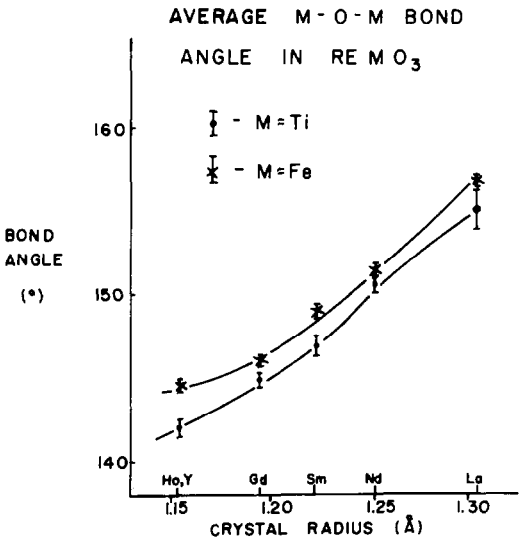

FIG. 4. Variation of the average Ti–O–Ti bond angle with the RE^{3+} crystal radius (*16*). Similar data for $REFeO_3$ are shown for comparison (*9,15*).

Acknowledgment

We acknowledge the National Research Council of Canada for support of this work. One of us (D. A. MacLean) is the recipient of a 1967 Science Scholarship also from the N.R.C. of Canada. We also thank Mr. J. D. Garrett for assistance in crystal growth, Mr. H. F. Gibbs for the neutron activation analysis, and Mr. R. Faggiani for assistance in collecting the X-ray data.

References

1. M. KESTIGIAN AND R. WARD *J. Amer. Chem. Soc.* **76**, 6027 (1954).
2. E. F. BERTAUT AND F. FORRAT, *J. Phys. Radium* **17**, 129 (1956).
3. W. D. JOHNSTON AND D. SESTRICH, *J. Inorg. Nucl. Chem.* **20**, 32 (1961).
4. H. HOLZAPFEL AND J. SIELER, *Z. Anorg. All. Chem.* **343**, 174 (1966).
5. P. GANGULY, O. PARKASH, AND C. N. R. RAO, *Phys. Status Solidi A* **36**, 669 (1976).
6. G. J. MCCARTHY, W. B. WHITE, AND R. ROY, *Mater. Res. Bull.* **4**, 251 (1969).
7. G. P. SHVEIKIN AND G. V. BAZUEV, *Russ. J. Inorg. Chem.* **18**, 155 (1973).
8. S. GELLER, *J. Chem. Phys.* **24**, 1236 (1956).
9. M. MAREZIO, J. P. REMEIKA, AND P. D. DERNIER, *Acta Crystallogr. Sect. B*, **26**, 2008 (1970).
10. J. E. GREEDAN AND D. A. MACLEAN, *Inst. Phys. Conf. Ser.*, No. 37, 249–254 (1978).
11. J. B. GOODENOUGH, *Progr. Solid State Chem.* **5**, 315 (1971).
12. D. T. CROMER AND J. T. WABER, *Acta Crystallogr.* **18**, 104 (1965).
13. D. T. Cromer, *Acta Crystallogr.* **18**, 17 (1965).
14. A. C. LARSON, *Act Crystallogr.* **23**, 664 (1967).
15. M. MAREZIO AND P. D. DERNIER, *Mater. Res. Bull.* **6**, 23 (1971).
16. R. D. SHANNON AND C. T. PREWITT, *Acta Crystallogr. Sect. B* **25**, 925 (1969).